Comparative Study of Phototactic and Photophobic Receptor Chromophore Properties in *Chlamydomonas reinhardtii*

David N. Zacks,*‡ Fadila Derguini,§ Koji Nakanishi,§ and John L. Spudich*‖

*Department of Anatomy and Structural Biology, Albert Einstein College of Medicine, Bronx, New York 10461 USA; §Department of Chemistry, Columbia University, New York, New York 10027 USA; ‖Department of Microbiology and Molecular Genetics, University of Texas Medical School, Houston, Texas 77030 USA

ABSTRACT The motile, unicellular, eukaryotic alga *Chlamydomonas reinhardtii* exhibits two distinct behavioral reactions to light stimuli, phototaxis and the photophobic response. Both are mediated by retinal-containing receptors. This paper focuses on a direct comparison of the two photoresponses and the chromophore requirements for their photoreceptor(s). Using computerized motion analysis assays for phototaxis and photophobic responses by the same populations of cells, we measured the ability of various isomers and analogues of retinal to reconstitute photobehavior in the pigment-deficient mutant FN68. The results indicate that photophobic and phototaxis responses each require chromophores with an all-*trans* polyene chain configuration, planar ionone ring/polyene chain conformation, and the ability to isomerize around the retinal C13–C14 double bond. One difference between the two behaviors is that the photophobic response becomes highly desensitized after light stimuli to which the phototaxis response does not become desensitized, indicating the existence of at least one distinct step in the photophobic response pathway. A second difference is that the retinal regeneration of the photophobic response but not of phototaxis is inhibited by a 5-membered ring 13-*trans*-locked analogue. While showing close similarity in the chromophore structural requirements of the two behaviors, the results indicate that differences exist between the two responses at the level of their photoreceptor proteins and/or in their transduction processes.

INTRODUCTION

The unicellular eukaryotic alga *Chlamydomonas reinhardtii* exhibits two behavioral reactions to light: the phototaxis response—orientation of swimming along the axis of the light stimulus (1)—and the photophobic response—a brief period of backward swimming after a rapid change in light intensity (2). Foster and coworkers (3) showed that retinal and retinal analogues restored phototaxis in the low-sensitivity, pigment-deficient mutant FN68 and that the wavelength of maximum sensitivity depended on the particular analogue added. These two features are characteristic of retinylidene (rhodopsin-like) proteins (4) and provided compelling evidence that a rhodopsin-like protein is the photoreceptor for phototaxis in *C. reinhardtii*. 11-*cis* Retinal was found to reconstitute higher sensitivity than all-*trans* retinal, and it was suggested that 11-*cis* is the native polyene chain configuration for the phototaxis photoreceptor's chromophore (3). Foster and coworkers (5) incorporated analogues which have their C6–C7 single bond locked in either the *cis*- or *trans*- planar conformation and obtained higher sensitivity with either analogue than with retinal. This suggested that in *vivo* the chromophore's ionone ring is coplanar with its polyene chain. Regiospecific isomerization of retinal (e.g., from 11-*cis* to all-*trans*, as is the case in visual pigments (6), or from all-*trans* to 13-*cis*, as is the case in archaebacterial rhodopsins (7)) was concluded not to be necessary, since analogues prevented from double bond isomerization were able to reconstitute phototaxis in FN68 cells (8, 9).

A second pigment-deficient mutant, strain CC2359, is insensitive to light stimuli, but photophobic responses with shifted action spectra are restored after the addition of retinal and retinal analogues (10–12), showing that the photophobic response is also mediated by a rhodopsin-like protein. All-*trans* retinal reconstituted the photophobic response in CC2359 cells most efficiently, followed by 13-*cis*, 11-*cis*, 9-*cis*, and 7-*cis* retinal (10, 11). Isomerization around the C13–C14 double bond was concluded to be required for the photophobic response in CC2359 since 13-*trans*-locked and 13-*cis*-locked retinal do not restore photophobic responses and yet do enter the retinal binding pocket since they competitively inhibit response reconstitution by all-*trans* retinal (11). Takahashi et al. (12) show more efficient reconstitution of phototaxis in CC2359 with all-*trans* retinal than with 11-*cis* retinal but do not reconstitute either photoresponse with 13-*trans*-locked or 13-*cis*-locked retinal.

The data indicating different properties for the chromophore requirements of *C. reinhardtii* rhodopsin(s) are difficult to compare for two reasons. First, different strains were used for the analysis of phototaxis (primarily FN68) versus the analysis of the photophobic response (CC2359). Second, different assays were used for monitoring the two behaviors. Foster and coworkers (3) used a population migration assay, whereas photophobic responses were analyzed by computerized motion analysis (11–13) and by a light scattering assay (10). This paper reports our simultaneous examination of retinal and retinal analogue reconstitution of both the phototaxis and the photophobic responses in *C. reinhardtii* strain FN68. We used a computerized videomicroscopic motion

Received for publication 21 September 1992 and in final form 8 February 1993.

Address reprint requests to Dr. J. L. Spudich.

‡*Present address*: Department of Microbiology and Molecular Genetics, University of Texas Medical School, Houston, TX 77030.

0006-3495/93/07/508/11 $2.00

analysis system to monitor both responses in the same population of cells, allowing for a more direct comparison of both photoresponses' chromophore requirements.

MATERIALS AND METHODS

Retinal isomers and analogues

All-*trans* retinal (Fig. 1) was purchased from Sigma Chemical Co. (St. Louis, MO). All other isomers and analogues were prepared as described in Lawson et al. (11). Isomers and analogues were purified by high-performance liquid chromatography on a Whatman (Meldstone, England) 25-cm Magnum 9 semipreparative silica gel column eluted with a hexane/ethyl acetate (95/5, v/v) solvent system at a 3.0 ml/min flow rate, roto-evaporated to dryness, and dissolved in methanol (high-performance liquid chromatography grade), and the solution was stored in the dark at −70°C under argon.

Strains and media

Behaviorally wild-type cells CC124 (mt⁻, nit1, nit2, agg1) were grown photosynthetically on high-salt medium (14) with trace elements (15) under constant illumination or on high-salt acetate (14) with trace elements in the dark. Strain FN68 was obtained from the *Chlamydomonas* Culture Center (Duke University) and grown on high-salt acetate with trace elements in the dark. All growth was on 1.5% agar plates at 25°C, and 10–16 day cultures were used in all experiments.

Gametogenesis was induced in nitrogen minimal medium (NMM) (16) in the dark. Cells were taken from plates and suspended in 10 ml of NMM to a concentration of 2×10^6 cells/ml and gently agitated overnight at 25°C on a New Brunswick G-76 Gyrotory water bath shaker on rotor setting 3 (New Brunswick Scientific, Edison, NJ). Retinal dissolved in methanol was added to the NMM cell suspension and incubated for the amount of time indicated in each experiment. The concentration of methanol never exceeded 0.2%.

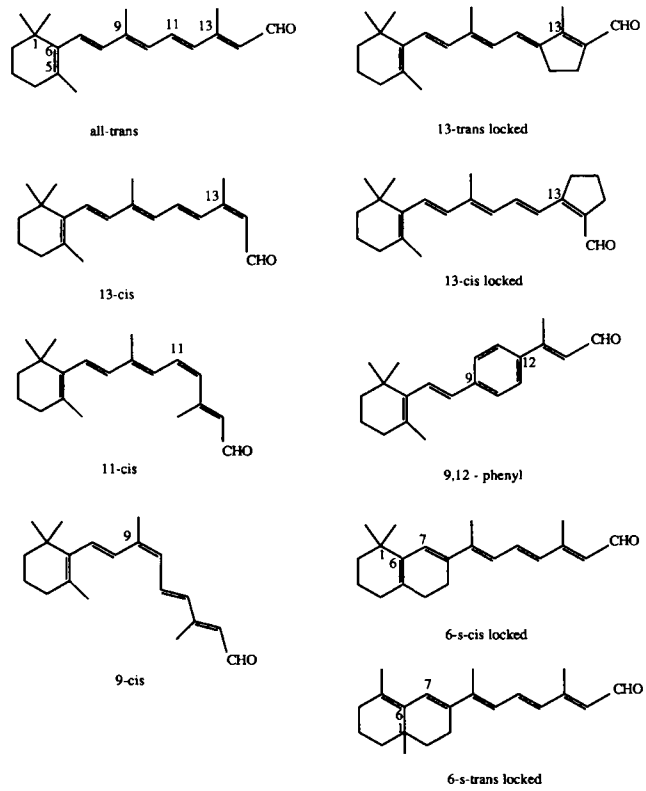

FIGURE 1 Retinal isomers and analogues.

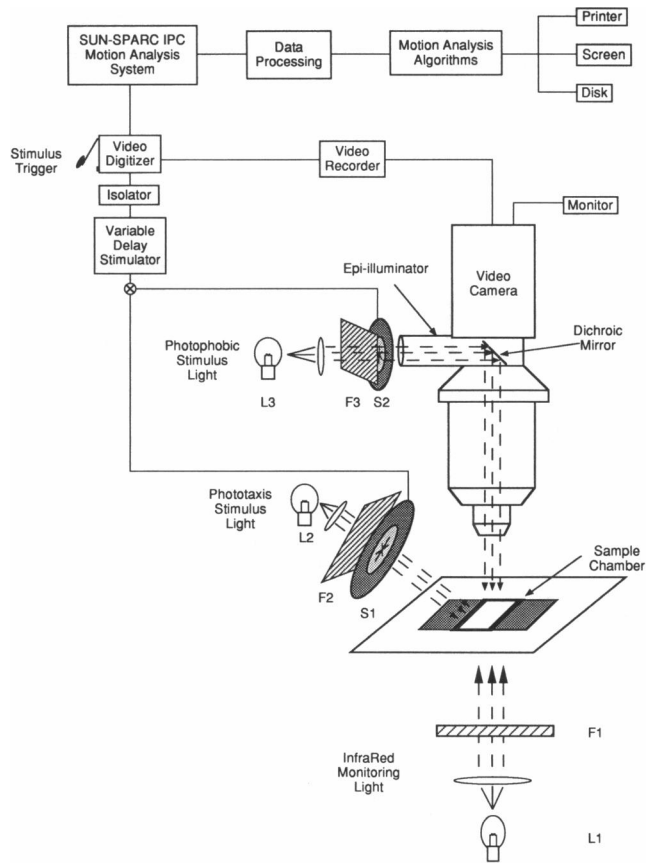

FIGURE 2 Optical arrangement for measurement of phototaxis and photophobic responses.

Behavioral assay

Photophobic stimuli were 200 ms in duration and were delivered via an epi-illuminator from the lamp designated L3 (Fig. 2). Phototaxis stimuli were 20 s in duration and were delivered via a fiber optic from lamp L2. The wavelength of both stimuli was 500 ± 20 nm (filters F2 and F3; Corion Corp., Holliston, MA). Cells were monitored by darkfield microscopy using nonactinic infrared light from lamp L1 (filter F1, 730–850 nm; Ditric Optics, Hudson, MA). All lamps were 100-W tungsten-halogen (Ushio, Inc., Tokyo, Japan), and intensity was controlled with neutral density filters (Corion Corp.). Pulse durations were controlled by electronic shutters (S1 and S2; Vincent Associates, Rochester, NY). The motion analysis system (Motion Analysis Corp., Santa Rosa, CA) was run on a SPARC IPC workstation (Sun Microsystems, Milpitas, CA) and received video input from the microscope via a charge-coupled device video camera (Cohu, Inc., San Diego, CA) and a VP-110 video digitizer (Motion Analysis Corp.). The shutters were triggered from the digitizer, and their delay was controlled by a pulse generator (Grass Instruments, Quincy, MA).

Algorithms for behavioral response analysis

Video data were collected at 15 frames/s (Fig. 3) and digitized using the Motion Analysis Corp. Expertvision software functions to generate a two-dimensional trace of the cells' swimming paths as a function of time. Only cells with an average speed greater than 20 μm/s were included for photobehavior analysis. This provides a lower-end cutoff for the exclusion of

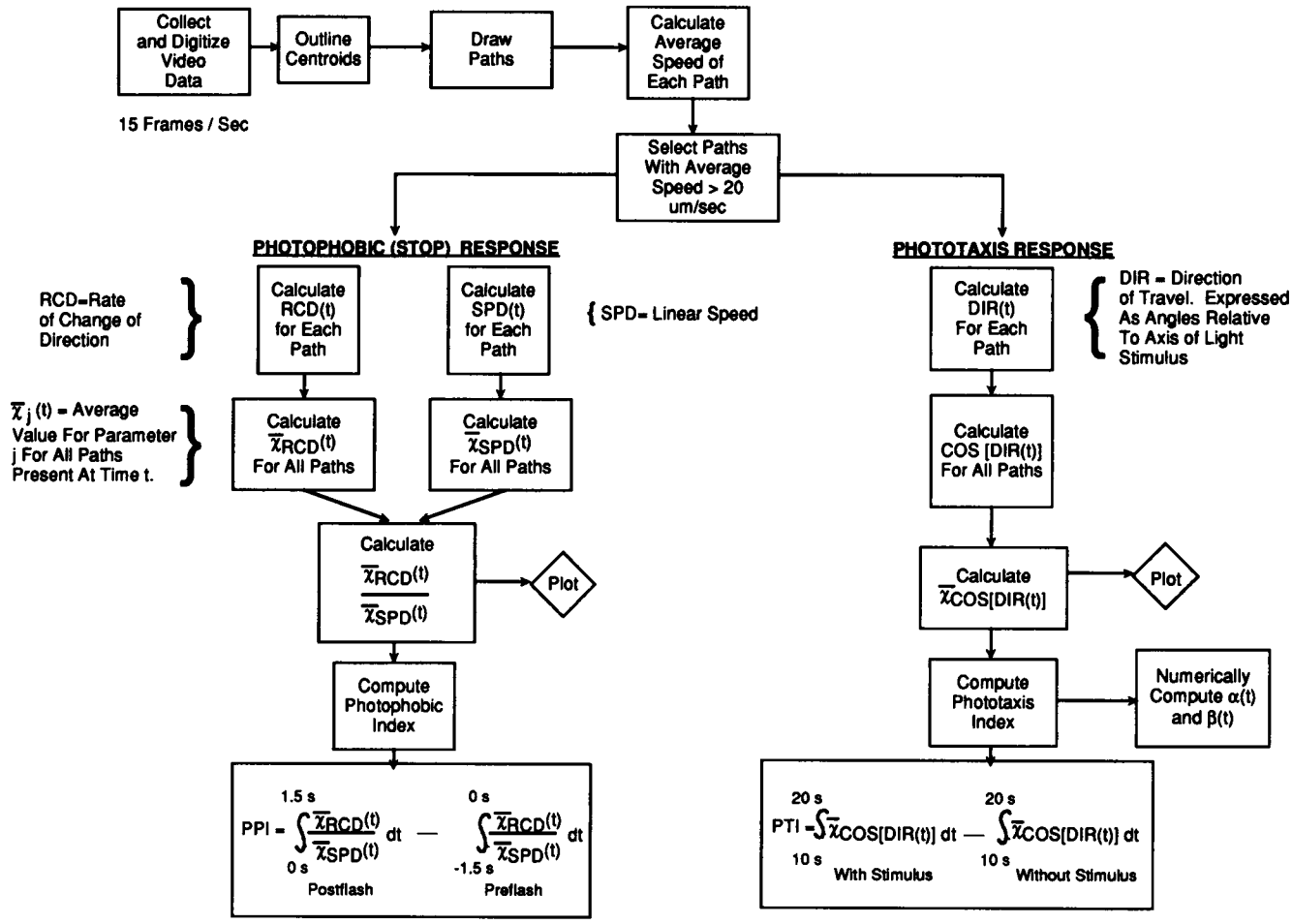

FIGURE 3 Algorithms for quantification of photobehavioral responses. See text.

nonmotile cells from the analysis. The average speeds for all populations examined were between 100 and 150 μm/s.

The algorithm for photophobic response analysis was essentially the same as described by Lawson et al. (11). Video data were collected for 3 s, and the selection process yielded approximately 300–500 cells/recording. Each cell's rate of change of direction and speed were calculated as functions of time (RCD(t) and SPD(t), respectively). The quotient of the population average RCD(t) and SPD(t) was taken as a measure of the photophobic response. After the addition of all-*trans* retinal to FN68, the quotient showed two peaks (data not shown), as described by Hegemann and Bruck (13) for wild-type cells and by Lawson et al. (11) for strain CC2359. The photophobic index in our analysis is the area under the curve for 1.5 s, beginning when the flash occurs, minus the area under the curve for 1.5 s prior to the flash (algorithm shown in Fig. 3). To allow a comparison of results from different populations, data for each experiment were normalized to the response obtained for that population of cells reconstituted with 20 nM all-*trans* retinal and stimulated with 3×10^4 erg/cm^2-s of 500-nm light. For every sample of cells six stimuli, separated by 10 s, were delivered. Unless specified elsewhere, the first photophobic recording of each cell sample was preceded by an identical photophobic stimulus, thus ensuring that cells in all recordings were exposed to at least one previous light stimulus.

Phototaxis responses were analyzed using the direction of travel (DIR) operator of the motion analysis software. This operator defines the angle the cell's path makes with the axis of the stimulating light. A cell swimming directly toward the light will define an angle of 0°, and a cell swimming directly away from the light will define an angle of 180°. The cosine of the direction of travel for each cell as a function of time (cos(DIR(t)) was taken and averaged together at each time point to yield a net measure of the population phototaxis response. If all the cells travel toward the light, the average cos(DIR(t)) = 1. Likewise, if all the of cells travel away from the light, the average cos(DIR(t)) = −1. An average cos(DIR(t)) = 0 can result from either of two conditions: the population is either swimming randomly or orienting symmetrically (e.g., half the population is orienting toward the light and the other half is orienting away from the light). We can distinguish between these conditions by examining the distribution of cosines at each time point and modeling this distribution by fitting it to a Beta function, as described in detail in the Appendix. Wild-type cells grown in the dark on acetate and FN68 cells reconstituted with all-*trans* retinal exhibit only negative phototaxis (data shown below), and therefore we calculate the phototaxis index as the area under the average cos(DIR(t)) curve for 10 s, beginning 10 s after the stimulus light was turned on, minus the area under the curve for 10 s of nonstimulus baseline.

Data for each phototaxis measurement were normalized to the response obtained for that population of cells reconstituted with 20 nM all-*trans* retinal and stimulated with 3×10^3 erg/cm^2-s of 500-nm light. For each cell sample four stimuli were delivered, separated by 30 s. Unless specified elsewhere, the first phototaxis recording of each cell sample in all experiments was preceded by an identical phototaxis stimulus. Each phototaxis response measurement included 1500–2000 paths.

RESULTS AND DISCUSSION

Phototaxis response quantitation

Fig. 4 shows the phototaxis response curves for two different populations of wild-type cells, each stimulated with an intensity of 3×10^3 erg/cm^2-s. Wild-type cells grown photo-

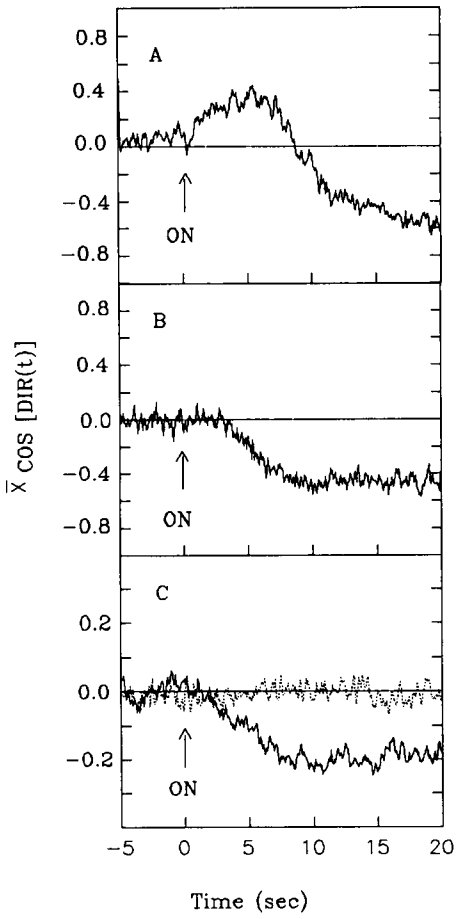

FIGURE 4 Phototactic response of (*A*) light-grown wild-type CC124 cells, (*B*) dark-grown wild-type CC124 cells, and (*C*) dark-grown FN68 cells with 20 nM all-*trans* retinal (*solid line*) or 20 μl methanol (*dotted line*). (*Abscissa*) Time after phototaxis stimulus initiation. (*Ordinate*) Mean cosine of the direction of travel for cell population.

synthetically under constant illumination responded to the light stimulus by first displaying positive and then negative phototaxis (Fig. 4 *A*). The initial positive response amplitude and duration increase as a function of time of incubation in NMM in the dark (data not shown). The crossover from positive to negative phototaxis does not represent randomization of orientation followed by a reorientation in the negative direction, but rather corresponds to the switching of individual cells from a positive to negative orientation response. This is shown both by the distribution of cosine values at the crossover point and by the Beta distribution (Appendix). Wild-type cells grown in the dark on acetate exhibited net negative phototaxis to the same stimulus (Fig. 4 *B*). Morel-Laurens (17) reported that titration of $[Ca^{2+}]$ extracellularly can mimic this phenomenon, with stronger initial positive response elicited with increased extracellular $[Ca^{2+}]$. The different phototaxis responses observed between light- and dark-grown wild-type cells here must be due to their different growth conditions, which perhaps causes a shift in the calcium-regulated set point controlling the direction of phototaxis response.

Reconstitution of phototaxis in FN68 cells

Cells of strain FN68 with 20 nM of all-*trans* retinal exhibited only negative phototaxis over all light intensities tested, as do the wild-type cells grown under the same conditions, but the final net population cosine value was approximately half that obtained in the wild-type cells (Fig. 4). Foster et al. (9) and Beckmann and Hegemann (18) reported a 1000-fold increase in the phototaxis sensitivity of FN68 cells, without exogenous retinal, after 20 min of exposure to 480-nm light. Our 20-s light stimulus does not induce this effect even after repeated exposure, and therefore our assay minimizes possible secondary effects of the light stimulus, which may cause response regeneration.

Reconstitution of photobehavior with retinal isomers: Evidence that the native polyene chain configuration for the phototaxis and photophobic response photoreceptor(s) in FN68 cells is all-*trans*

Cells were incubated with concentrations of retinal ranging from 0.2 to 40 nM, aliquots of each population were tested for their phototaxis response, and separate aliquots from the same population were tested for their photophobic response. Dose-response curves for the reconstitution of the photophobic and the phototaxis responses with all-*trans* retinal were indistinguishable (Fig. 5).

A comparison of the all-*trans* retinal reconstitution of photobehavior with the reconstitution capabilities of the 13-*cis*, 11-*cis*, and 9-*cis* isomers of retinal is shown in Fig. 6. The photophobic response was fully reconstituted by 2 nM all-*trans* retinal within 60 min, whereas 11-*cis* and 9-*cis* retinal did not reconstitute the response in this period (Fig. 6 *A*). Phototaxis was fully reconstituted by 2 nM all-*trans* retinal within 20 min, and the 11-*cis* retinal produced 40% reconstitution after 60 min (Fig. 6 *A, inset*). We did not detect any reconstitution of phototaxis after incubation with 9-*cis* retinal. To compare the reconstitution of photobehavior by all-*trans* and 13-*cis* retinal we lowered the concentration of isomer to 0.2 nM, since the two time courses were indistinguishable at 2 nM. All-*trans* retinal reconstituted the photophobic response to 20% of maximum after 60 min of incubation, during which the 13-*cis* retinal did not reconstitute the photophobic response (Fig. 6 *B*). Both isomers reconstituted phototaxis, but all-*trans* retinal was more effective (Fig. 6 *B, inset*).

The reconstitution data strongly suggest that the native chromophore(s) for both phototaxis and photophobic reception has an all-*trans* polyene chain configuration. The differences between the percentage reconstitution of the phototaxis and photophobic responses by *cis* isomers derives from the longer duration of the phototaxis stimulus (20 s) compared to the photophobic stimulus (200 ms), as shown for 11-*cis* retinal in Fig. 7. Cells were reconstituted with either 11-*cis* or all-*trans* retinal for 60 min and then exposed to four 20-s phototaxis stimuli of 3×10^3 erg/cm^2-s separated by 60 s. Seven seconds after each phototaxis stimulus, the cells were exposed to a 200-ms photophobic stimulus of 3 ×

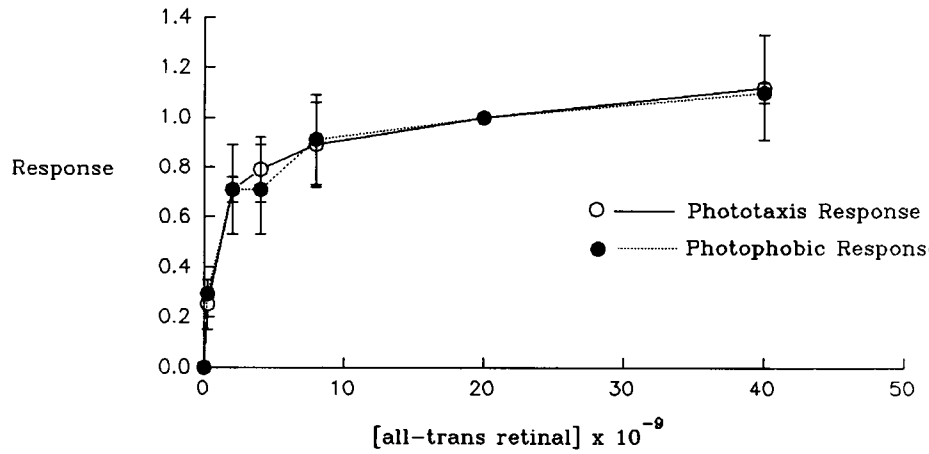

FIGURE 5 Dose-response curve for phototaxis and photophobic responses in FN68 cells incubated overnight with various concentrations of all-*trans* retinal. Stimulus intensity was 3×10^3 erg/cm^2-s. All data are normalized to the response obtained with 20 nM, as described in Materials and Methods.

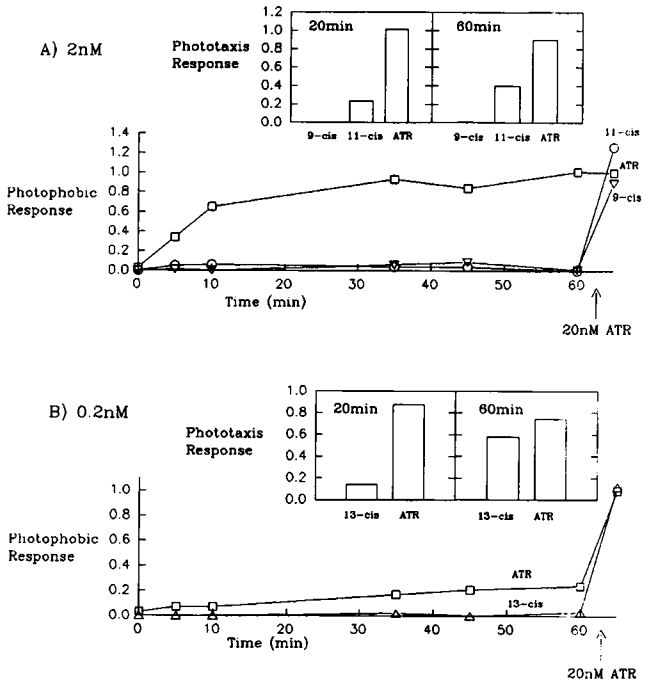

FIGURE 6 (*A*) Reconstitution of photophobic response in FN68 cells as a function of time after addition of 2 nM 9-*cis*, 11-*cis* or all-*trans* retinal (*ATR*). (*Inset*) Phototaxis response 20 or 60 min after the addition of each retinal isomer. (*B*) Same as (*A*) except that the 13-*cis* and all-*trans* retinal are added at a 0.2 nM concentration. Stimulus intensity and normalization as in Fig. 5.

10^4 erg/cm^2-s, delivered via the epi-illuminator. Cells reconstituted with all-*trans* retinal showed a decrease in their photophobic response after four photophobic response stimuli (see Desensitization, below). In contrast, cells reconstituted with 11-*cis* retinal, which showed no photophobic response after 60 min in the dark, had increased photophobic responses after each phototaxis stimulation. This indicates that a light-dependent process, perhaps chromophore isomerization, accounts for the phototaxis reconstitution observed with 11-*cis* retinal in Fig. 6.

The 6-s-*trans*-locked retinal analogue (Fig. 1) reconstituted both photoresponses to approximately 50% of the all-*trans* reconstituted value, but the 6-s-*cis*-locked retinal analogue did not reconstitute either photoresponse after an 18-h incubation (data not shown), suggesting that in the receptor(s) the β-ionone ring is *trans* with respect to the polyene chain.

Response reconstitution with retinal analogues

The 13-*trans*-locked and the 13-*cis*-locked retinals are prevented from isomerizing around the C13–C14 double bond by the presence of a five-membered ring. We do not detect any reconstitution of the photophobic or the phototaxis

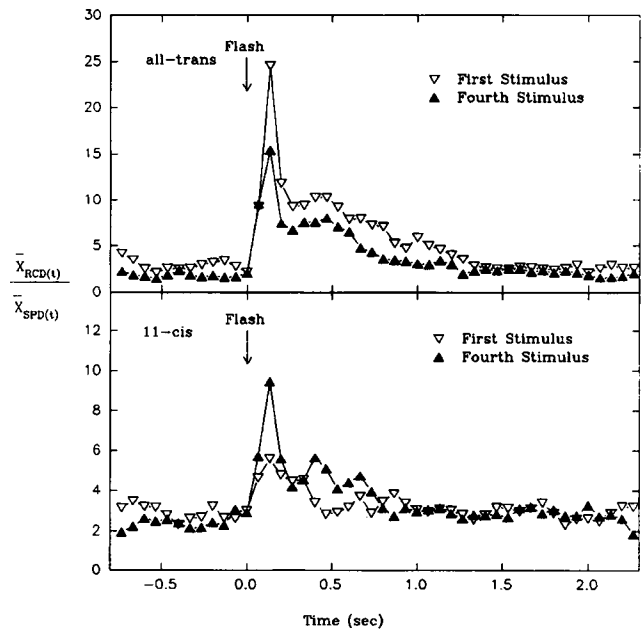

FIGURE 7 Photophobic responses of FN68 cells incubated, in the dark, with either all-*trans* or 11-*cis* retinal for 1 h. The first stimulus (▽) was given 7 s after a 20-s exposure to the phototaxis stimulus, and the fourth stimulus (▲) was given 7 s after the fourth 20-s phototaxis stimulus. Phototaxis stimuli were separated by 60 s, and the first phototaxis stimulus did not have a pre-exposure to the stimulus. (*Abscissa*) Time after photophobic flash. (*Ordinate*) Ratio of the mean population rate of change of direction and the mean population speed.

responses in FN68 after overnight incubation with these analogues (data not shown). Cells were incubated with analogue concentrations of 2, 20, 80, and 400 nM and stimulated with intensities ranging from 3×10^1 to 1×10^4 erg/cm^2-s for the phototaxis response and from 1×10^2 to 2×10^4 erg/cm^2-s for the photophobic response. Another analogue with hindered isomerization, 9,12-phenyl retinal, was added to cell suspensions in 40 and 400 nM concentrations and did not reconstitute either photoresponse.

Inhibition of photobehavior by 13-*trans*-locked retinal

We tested the inhibition of all-*trans* retinal reconstitution of photophobic and phototaxis responses by incubating FN68 cells with 2 nM all-*trans* retinal together with various concentrations of 13-*trans*-locked retinal. Light stimulation was in the linear range of the fluence response curve and was verified for each population of cells. All-*trans* retinal reconstitution was inhibited by up to 40% by the locked analogue, but there was no effect of analogue on the restoration of the phototaxis response (Fig. 8, *top*). Fig. 8 (*middle* and *bottom*, respectively) shows the photophobic and phototaxis response curves for FN68 cells coincubated with 2 nM all-*trans* retinal and 20 nM 13-*trans*-locked retinal. The photophobic response is reduced by 20%, whereas the phototaxis response is not reduced. Lowering the all-*trans* retinal concentration to 1 nM resulted in an increased level of photophobic response inhibition, saturating at approximately 70% inhibition (data not shown). Since the extent of inhibition exhibits saturation, a simple competitive inhibition scheme (11) may not fit the data at high concentrations of inhibitor. This would indicate departure from the conditions required for competitive inhibition, as delineated in Lawson et al. (11).

Desensitization

Phototaxis and photophobic responses differ in their responses to repetitive light stimuli. Phototaxis responses of reconstituted FN68 cells to the first and to the fourth of consecutively delivered 20-s stimuli are nearly superimposable, indicating that no desensitization has occurred (Fig. 9, *top*).

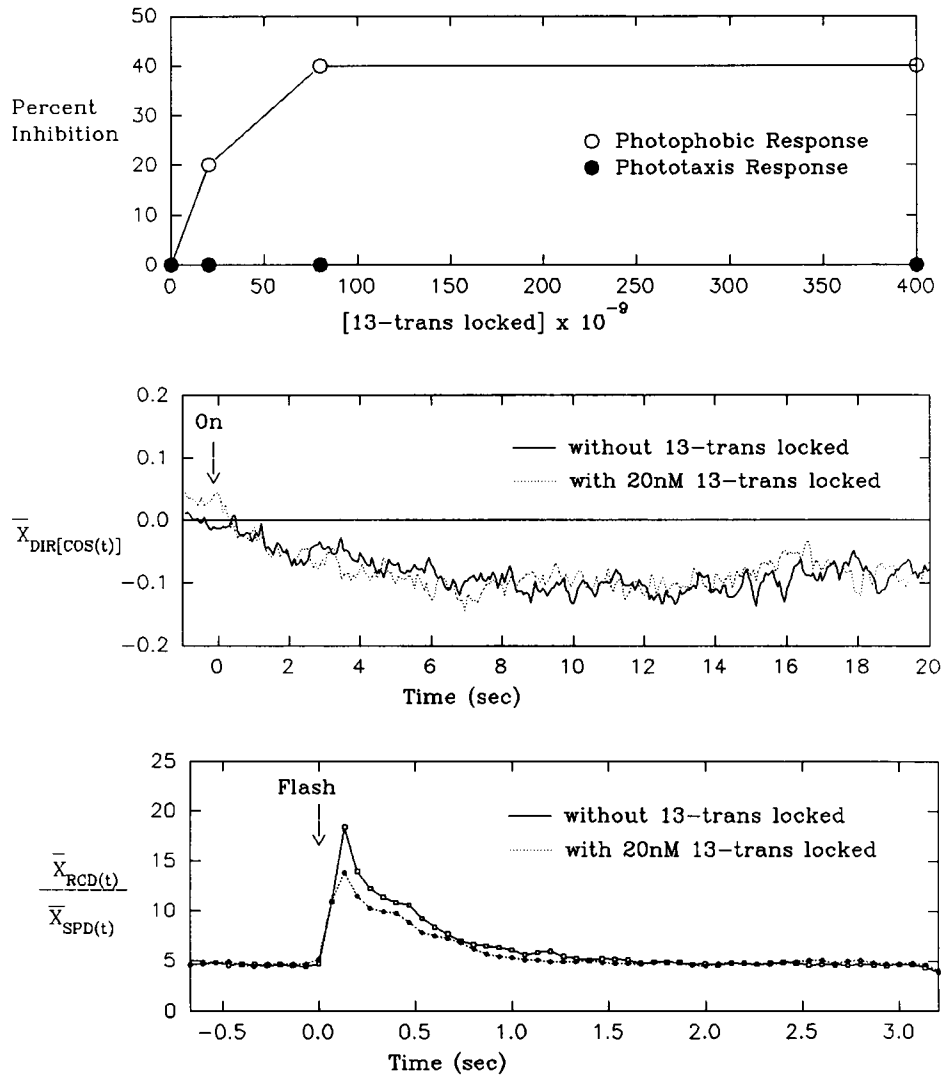

FIGURE 8 Inhibition of all-*trans* retinal (2 nM) reconstitution of photobehavior in FN68 cells with 13-*trans* locked retinal. (*Top*) Inhibition of phototaxis and photophobic responses as a function of 13-*trans* locked retinal concentration. (*Middle*) Phototaxis in FN68 cells coincubated with analogue (*solid line*) versus cells only incubated with all-*trans* retinal (*dotted line*). (*Bottom:*) Photophobic responses in FN68 cells coincubated with analogue (*solid line*) versus cells only incubated with all-*trans* retinal (*dotted line*).

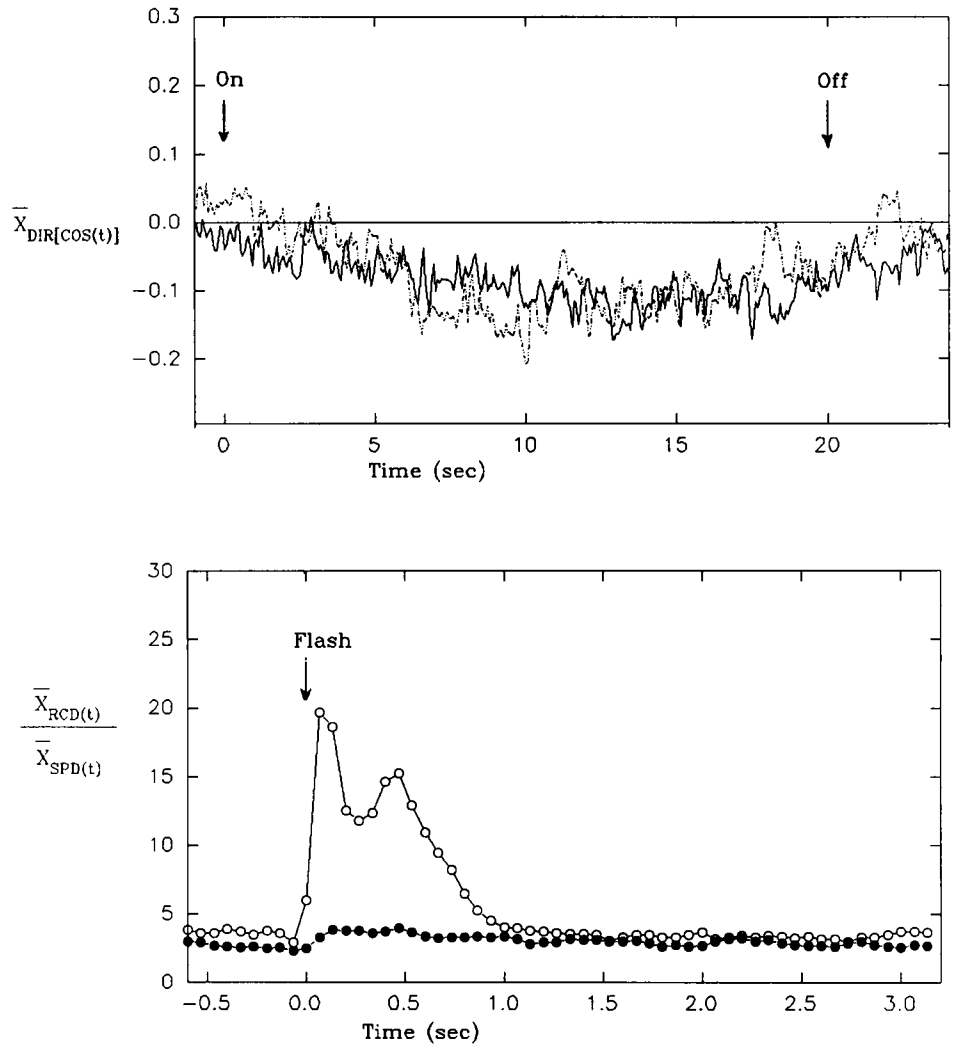

FIGURE 9 Desensitization of photophobic and phototaxis responses in FN68 cells reconstituted with 20 nM all-*trans* retinal. (*Top*) Phototaxis responses to the first (*solid line*) versus the fourth (*dotted line*) of four consecutive 20-s stimuli each separated by 30 s. (*Bottom*) Photophobic responses in the same cells as in the top panel to the onset of the phototaxis stimuli.

In contrast, nearly total desensitization is observed in the photophobic response to onset of the same photostimuli (Fig. 9, *bottom*). Photophobic responses were measured 10 s after various durations at three different intensities of preillumination (Fig. 10) and the extent of desensitization closely matches the fluence response curve of the photophobic response. The curves fit well a two-exponential process with one positive and one negative rate constant (Fig. 10), suggesting a competitive process between the light-induced decrease in sensitivity and a second process maintaining sensitivity. Cells recovered photophobic sensitivity from their maximally adapted state slowly, with only 50% of response recovered after 60 s (Fig. 11).

SUMMARY AND CONCLUSIONS

Direct comparison of the chromophore requirements for the reconstitution of phototaxis and photophobic responses in *C. reinhardtii* strain FN68 indicates that both responses require an all-*trans* polyene chain configuration and a 6-s-*trans* conformation. These properties match those found for the photophobic response in strain CC2359 (10, 11) and for archaebacterial rhodopsins (21). Retinal extracted from light-exposed FN68 cells is predominantly all-*trans* (19), and Takahashi et al. (12) reported a higher final phototaxis response in CC2359 cells after reconstitution with all-*trans* retinal than with 11-*cis* retinal. Our reconstitution data for strain FN68 are consistent with these reports. However, Foster and coworkers (3) reported a higher sensitivity after reconstitution of FN68 cells with 11-*cis* retinal than with all-*trans* retinal. As noted by Hegemann et al. (10), Foster's group used high retinal concentrations (25 μM), and even trace levels of all-*trans* retinal contamination would be sufficient to reconstitute phototaxis. Phototaxis response saturation in FN68 occurs with 10 nM all-*trans* retinal (Fig. 5), and it would require only a 0.04% all-*trans* isomer in the 11-*cis* preparation to yield high levels of response. An additional factor that may influence the results is evident from our observation that the 20-s phototaxis stimulating light enhances the reconstitution of the photophobic response with 11-*cis* retinal, whereas the 200-ms photophobic stimulation does not (Fig. 7). Foster et al. (3) stimulate the cells for 600

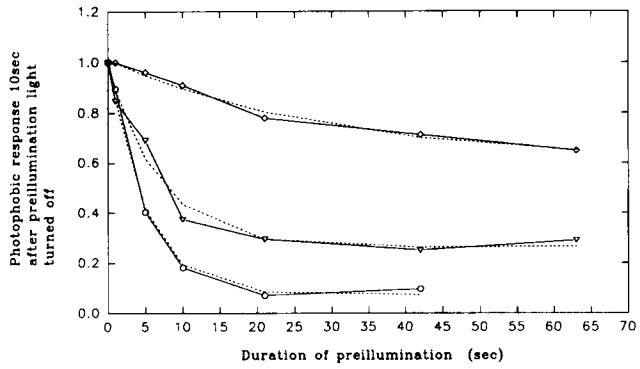

FIGURE 10 Photophobic responses of FN68 cells reconstituted with 20 nM all-*trans* retinal and exposed to various durations of preillumination. Preillumination was at 500 ± 20 nm and was delivered via the phototaxis stimulus lamp L2. A 200-ms saturating photophobic stimulus was delivered 10 s after the preillumination ends via lamp L3. Each point is the average of 6 photophobic responses. Preillumination intensities were: 2×10^4 erg/cm^2-s (○); 3×10^3 erg/cm^2-s (▽); 2×10^2 erg/cm^2-s (◇). Dotted lines are from double exponential fits to the data. The equation used for curve fitting was $y = a_1 \exp(-b_1 x) + a_2 \exp(-b_2 x)$. The coefficients for a_1, b_1, a_2, and b_2, starting with the highest preillumination intensity, are 1.01, 0.188, 0.021, and −0.036; 0.800, 0.121, 0.180, and −0.010; and 0.478, 0.030, 0.534, and −0.001, respectively. Response normalized as in Fig. 5.

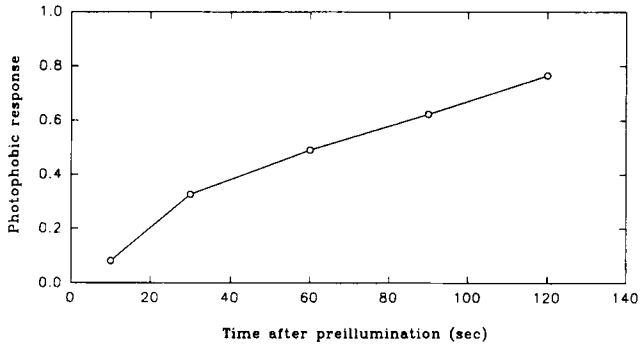

FIGURE 11 Rate of return of photophobic sensitivity to FN68 cells reconstituted with 20 nM all-*trans* retinal after the end of preillumination. Preillumination intensity was 2×10^4 erg/cm^2-s. Photophobic stimuli were the same as in Fig. 10. Stimulus intensity and normalization as in Fig. 5.

s, which may provide sufficient chromophore availability for phototaxis response reconstitution through a secondary light-dependent process. 11-*cis* Retinal has very little extinction at 500 nm, so such a secondary process would require a reconstitution intermediate or a second retinal-binding protein absorbing at longer wavelengths than free retinal.

The absence of reconstitution of the photobehavior by 13-locked analogues indicates that for both photoresponses receptor activation requires isomerization across the C13–C14 double bond. Inhibition of all-*trans* regeneration of the photophobic response by the 13-*trans*-locked analogue indicates that the analogue enters the chromophore binding pocket. The inhibition experiments were conducted in the linear ranges of the fluence-response curves for both sensitivities in which a decrease in the light intensity yields a decrease in the photophobic and phototaxis responses. Inhibition of the photoreceptor is expected to mimic the effect of decreasing the light intensity and thereby result in a decreased response. The lack of inhibition of the phototaxis response therefore is a significant difference in the two behavioral systems. One possible explanation is the existence of a second rhodopsin, with a different retinal binding pocket, controlling the phototaxis response. A second possibility is that the same opsin is involved in both responses, as suggested by Takahashi et al. (12), but that they are localized differently within the cell, so that all-*trans* retinal, but not 13-*trans*-locked retinal, can access the receptors involved in phototaxis, perhaps by an isomer-specific chromophore transporter. A third possibility is that the same opsin in the same location mediates both responses but that a compensatory mechanism increases the gain on the phototaxis sensitivity to compensate for the decrease in functional photoreceptor. Such a mechanism might be similar to the bleaching adaptation observed in tiger salamander rhodopsin (20) and may help explain the different adaptation properties for the two responses. The different desensitization properties of the two photobehaviors demonstrate at least one point of divergence between the two responses' sensory transduction pathways.

APPENDIX

Derivation of the distribution of $Y = \cos(\Theta)$ in the dark

Let Θ be the orientation angle (in radians) of a cell's swimming direction relative to the axis of the phototaxis light stimulus. In the dark Θ is a random variable with a uniform distribution over the interval $(-\pi, \pi)$ (data not shown). The probability density function of Θ is

$$f(\Theta) = \begin{cases} 1/2\pi, & \text{if } -\pi \le \Theta \le \pi \\ 0, & \text{otherwise.} \end{cases}$$

Let $Y = \cos(\Theta)$. Y is a random variable assuming values in the interval $[-1, 1]$. To derive the probability density function of Y, we define $\cos^{-1}(y)$, for $-1 \le y \le 1$, to be the unique inverse image of $y = \cos(\Theta)$ over the interval $0 \le \Theta \le \pi$. Notice that

$$\frac{d}{dy}\{\cos^{-1}(y)\} = -\frac{1}{(1 - y^2)^{-1/2}}, \qquad -1 < y < 1.$$

The cumulative distribution function of Y is, for each $-1 < y < 1$,

$$F(y) = P_r\{Y \le y\}$$
$$= P_r\{\Theta \le -\cos^{-1}(y)\} + P_r\{\Theta \ge \cos^{-1}(y)\}.$$

From the above assumption on the uniform distributions of Θ over $(-\pi, \pi)$,

$$P_r\{\Theta \le \theta\} = \frac{\theta + \pi}{2\pi} = \frac{1}{2} + \frac{\theta}{2\pi}, \qquad -\pi \le \theta \le \pi.$$

Hence,

$$F(y) = 1 - \{(1/\pi)\cos^{-1}(y)\}$$

Finally, the probability density of Y is obtained by differentiating $F(y)$,

$$f_Y(y) = (1/\pi)(1 + y)^{-1/2}(1 - y)^{-1/2}, \qquad -1 \le y \le 1$$

General modeling

The family of probability densities

$$f(y; \alpha, \beta) = \{1/B(\alpha,\beta)\}(1 + y)^{\alpha-1}(1 - y)^{\beta-1},$$

$$-1 \le y \le 1 \quad \text{and} \quad 0 < \alpha, \quad \beta < \infty$$

where $B(\alpha, \beta) = u^{\alpha-1}(1 - u)^{\beta-1}\,du$ (called the Beta function) includes the density of $Y = \cos(\Theta)$ in the case where $\alpha = \beta = 0.5$. This family of probability densities can be used to describe the distributions of Y observed under various light conditions. Notice that $U = (1 + Y)/2$ is distributed over (0, 1), and the family of densities

$$g(u; \alpha, \beta) = \{1/B(\alpha,\beta)\}u^{\alpha-1}(1 - u)^{\beta-1}, \qquad 0 \le u \le 1$$

is called the Beta family of probability densities.

Estimating the parameters α, β by the Method of Moments

Suppose that $y_1, \ldots, y_n$ is a sample of n Y values obtained under some light condition. Let $u_i = (1 + y_i)/2$, $i = 1, \ldots, n$. $u_1, \ldots, u_n$ can be considered as a sample from the Beta distribution, with parameters α and β. The first two sample moments are

$$M_1 = \frac{1}{n}\Sigma\, u_i$$

$$M_2 = \frac{1}{n}\Sigma\, u_i^2$$

Notice that since $0 < u < 1$, $u^2 < u$ and $M_2 < M_1$. On the other hand $M_2 > M_1^2$. $S^2 = M_2 - M_1^2$ is the sample variance.

The theoretical moments of first and second order of the Beta(α,β) distribution are

$$u_1 = \frac{\alpha}{\alpha + \beta}$$

and

$$u_2 = \frac{\alpha(\alpha + 1)}{(\alpha + \beta)(\alpha + \beta + 1)}$$

The Method of Moments estimates of α and β are obtained by solving the equations

$$M_1 = \frac{\alpha}{\alpha + \beta}$$

$$M_2 = \frac{\alpha(\alpha + 1)}{(\alpha + \beta)(\alpha + \beta + 1)}$$

Simple algebraic operations yield the formulae

$$\alpha = \frac{M_1(M_1 - M_2)}{S^2}$$

$$\beta = \frac{\alpha(1 - M_1)}{M_1}$$

Positive versus negative phototaxis

To separate the positively and negatively orienting cells in the population shown in Fig. 4 *A*, we analyzed the distribution of cosines. At each time point, the distribution of cosines can be closely approximated by the Beta distribution as described above. Fig. 12 shows the observed cosine distribution for the paths in Fig. 4 *A*, prior to stimulation, versus the Beta distribution with α and β values experimentally derived for that population by the method of moments. This bimodally shaped curve is expected from the Beta distribution function $f_Y(y) = (1/\pi)(1 + y)^{-1/2}(1 - y)^{-1/2}$, $-1 \le y \le 1$. Fig. 13 shows the observed versus calculated frequency distributions for the population when it is exhibiting only negative phototaxis. The goodness of fit for the two distributions is tested by calculating the proportion negative for the observed and the calculated frequencies. For both the phototaxing and nonphototaxing populations these values differ by less than 4%. Although the Beta distribution calculation introduces a greater skew than the actual data, the parameters α and β are functions of the number of cells

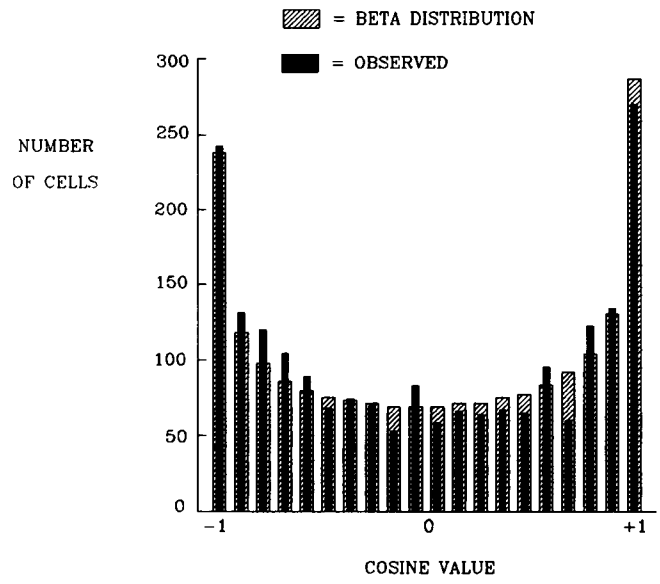

FIGURE 12 Distribution of cosine values of the direction of travel of cells in a randomly swimming population of wild-type cells (*solid bars*) versus the distribution of cosines calculated from the Beta distribution with parameters $\alpha = 0.57$ and $\beta = 0.53$.

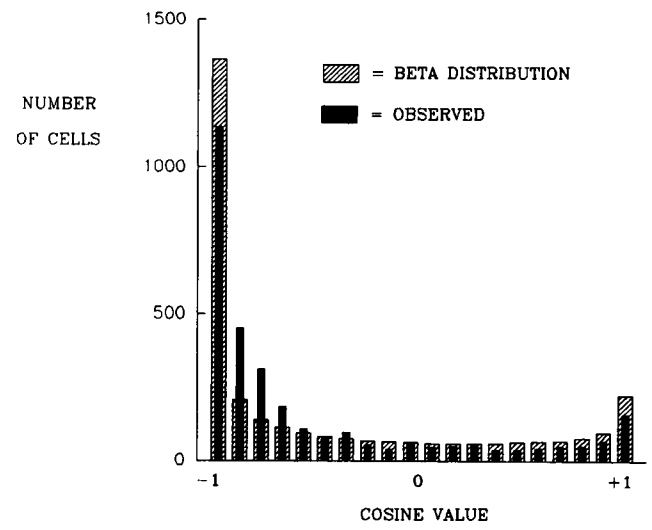

FIGURE 13 Distribution of cosine values of the direction of travel of cells in a negatively phototaxing population of wild-type cells (*solid bars*) versus the distribution of cosines calculated from the Beta distribution with parameters $\alpha = 0.16$ and $\beta = 0.49$.

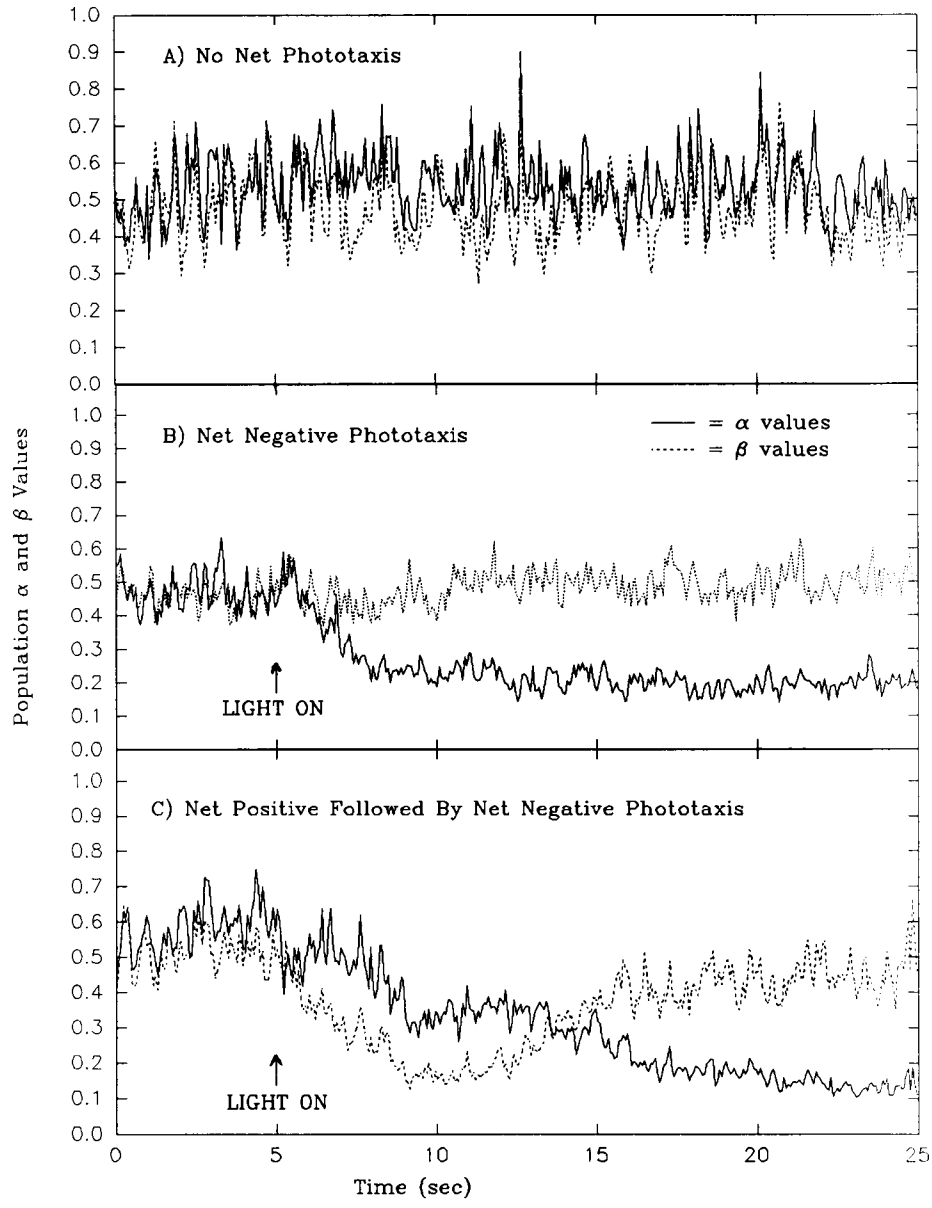

FIGURE 14 (*A*) α and β values as a function of time for a population of wild-type cells in the dark. (*B*) α and β values as a function of time for a population of wild-type cells exhibiting net negative phototaxis. (*C*) α and β values as a function of time for a population of wild-type cells exhibiting net positive followed by net negative phototaxis.

swimming away from or toward the light, respectively, and can therefore be used as indices of the negative and positive phototaxis response. Fig. 14 shows the α and β values as a function of time for the same populations as shown in Fig. 4. The final α and β values are approximately the same for both populations, but the kinetics of the population responses differ. In the light-grown population there is an initial positive phototaxis response, resulting in a decreased β value which then returns to its initial value as the population switches to net negative phototaxis. The dark-grown population exhibits only net negative phototaxis from the onset of the stimulus and thus shows a change only in its α values. The lower β values during the initial positive phototaxis response of the light-grown cells define a cosine distribution skewed toward +1. The switch point from positive to negative phototaxis is represented by α and β values lower than those found during the prestimulus condition. These values define a cosine distribution that is bimodal but skewed more toward both extremes than in the prestimulus condition, demonstrating that the cells are not randomly oriented but that half are exhibiting positive and half-negative phototaxis.

We wish to thank Dr. Shelley Zacks of the Department of Mathematical Sciences at the State University of New York at Binghamton for his help with the statistical analysis. We also wish to thank Dr. Jeffrey Segall of the Department of Anatomy and Structural Biology at the Albert Einstein College of Medicine for his helpful discussions regarding the motion analysis. This investigation was supported (in part) by National Science Foundation grant MCB-9219854 and NIH training grant T32 GM07288 from the National Institute of General Medical Sciences.

REFERENCES

1. Feinleib, M., and G. Curry. 1967. Methods for measuring phototaxis of cell populations and individual cells. *Physiol. Plant.* 20:1083–1095.
2. Ringo, D. 1967. Flagellar motion and fine structure of the flagellar apparatus in *Chlamydomonas*. *J. Cell Biol.* 33:543–571.
3. Foster, K., J. Saranak, N. Patel, G. Zarrilli, M. Okabe, T. Kline, and K. Nakanishi. 1984. A rhodopsin is the functional photoreceptor for phototaxis in the unicellular eukaryote *Chlamydomonas*. *Nature (Lond.).* 311:756–759.
4. Balogh-Nair, V., and K. Nakanishi. 1990. Visual pigment and bacteriorhodopsin analogs. *In* Chemistry and Biology of Synthetic Retinoids. M. Dawson and W. Okamura, editors. CRC Press, Boca Raton, FL. 147–176.

5. Foster, K., J. Saranak, R. van der Steen, and J. Lugtenburg. 1987. Retinal in *Chlamydomonas* rhodopsin is in a planar 6-s-*trans* conformation as shown by *in vivo* incorporation of 6–7 locked retinal analogs. *Invest. Optham. Vis. Sci.* a28(supplement):S253.
6. Birge, R. 1990. Nature of the primary photochemical events in rhodopsin and bacteriorhodopsin. *Biochim. Biophys. Acta.* 1016:293–327.
7. Yan, B., T. Takahashi, R. Johnson, F. Derguini, K. Nakanishi, and J. L. Spudich. 1990. All-*trans*/13-*cis* isomerization of retinal is required for phototaxis signaling by sensory rhodopsins in *Halobacterium halobium. Biophys. J.* 57:807–814.
8. Foster, K., J. Saranak, F. Derguini, J. Rao, G. Zarrilli, M. Okabe, J. Fang, N. Shimizu, and K. Nakanishi. 1988. Rhodopsin activation: a novel view suggested by *in vivo Chlamydomonas* experiments. *J. Am. Chem Soc.* 110:6588.
9. Foster, K., J. Saranak, F. Derguini, G. Zarrilli, R. Johnson, M. Okabe, and K. Nakanishi. 1989. Activation of *Chlamydomonas* rhodopsin *in vivo* does not require isomerization of retinal. *Biochemistry.* 28:819–824.
10. Hegemann, P., W. Gartner, and R. Uhl. 1991. All-*trans* retinal constitutes the functional chromophore in *Chlamydomonas* rhodopsin. Biophys. J. 60:1477–1489.
11. Lawson, M., D. N. Zacks, F. Derguini, K. Nakanishi, and J. L. Spudich. 1991. Retinal analog restoration of photophobic responses in a blind *Chlamydomonas reinhardtii* mutant: evidence for an archaebacterial-like chromophore in a eukaryotic rhodopsin. *Biophys. J.* 60:1490–1498.
12. Takahashi, T., Y. Kazuao, W. Masakatsu, M. Kubota, R. Johnson, F. Derguini, and K. Nakanishi. 1991. Photoisomerization of retinal at 13-ene is important for phototaxis of *Chlamydomonas reinhardtii:* simultaneous measurements of phototactic and photophobic responses. *Biochem. Biophys. Res. Commun.* 178:1273–1279.
13. Hegemann, P., and B. Bruck. 1989. Light-induced response in *Chlamydomonas reinhardtii:* occurrence and adaptation phenomena. *Cell Motil. Cytoskeleton.* 14:501–515.
14. Sueoka, N. 1960. Mitotic replication of deoxyribonucleic acid in *Chlamydomonas reinhardtii. Proc. Nat. Acad. Sci. USA.* 46:83–91.
15. Hutner, S., L. Provasoli, A. Schatz, and C. Haskins. 1950. Some approaches to the study of the role of metals in the metabolism of microorganisms. *Proc. Am. Philos. Soc.* 94:152–170.
16. Sears, B., J. Boynton, and H. Gillheam. 1980. The effect of gametogenesis regimes on the chloroplast genetic system of *Chlamydomonas reinhardtii. Genetics* 96:95–114.
17. Morel-Laurens, N. 1987. Calcium control of phototactic orientation in *Chlamydomonas reinhardtii*: sign and strength of response. *Photochem. Photobiol.* 45:119–128.
18. Beckmann, M., and P. Hegemann. 1991. *In vitro* identification of rhodopsin in the green alga *Chlamydomonas. Biochemistry.* 30:3692–3697.
19. Derguini, F., P. Mazur, K. Nakanishi, D. M. Starace, J. Saranak, and K. W. Foster. 1991. All-trans retinal is the chromophore bound to the photoreceptor of the alga *Chlamydomonas reinhardtii. Photochem. Photobiol.* 54:1017–1021.
20. Corson, D., M. Cornwall, E. MacNichol, J. Jin, R. Johnson, F. Derguini, R. Crouch, and K. Nakanishi. 1990. Sensitization of bleached rod photoreceptors by 11-cis-locked analogues of retinal. *Proc. Natl. Acad. Sci. USA.* 87:6823–6827.
21. Bogomolni, R. A., and J. L. Spudich. 1991. Archaebacterial rhodopsins: sensory and energy transducing membrane proteins. *In* Modern Cell Biology. Vol. 10. J. L. Spudich and B. Satir, editors. Wiley-Liss, Inc., New York. 227–249.
22. Foster, K., J. Saranak, and G. Zarrilli. 1988. Autoregulation of rhodopsin synthesis in *Chlamydomonas reinhardtii. Proc. Natl. Acad. Sci. USA.* 85:6379–6383.